

# Study of $\psi' \rightarrow \Lambda \bar{\Lambda} \omega$ at BESIII

## Abstract

Based on  $4.48 \times 10^8$   $\psi'$  events collected with BESIII detector at BEPCII, we present the measurement of  $\psi' \rightarrow \Lambda \bar{\Lambda} \omega$ , which is observed for the first time. The branching fraction is measured to be  $(3.42 \pm 0.34(stat.) \pm 0.31(syst.)) \times 10^{-5}$ . There is no evidence of any  $\Lambda^*$  in both and mass distributions. However a 2-dimesional fit to the Dalitz plot of  $\psi' \rightarrow \Lambda \bar{\Lambda} \omega$  gives a mass of  $2.001 \pm 0.007 \text{ GeV}/c^2$  and width is  $0.036 \pm 0.014 \text{ GeV}/c^2$  with the significance of  $3.3\sigma$ . The corresponding upper limit branching fraction of  $B(\psi' \rightarrow \Lambda \bar{\Lambda}^*/\bar{\Lambda} \Lambda^* \rightarrow \Lambda \bar{\Lambda} \omega)$  is estimated to be  $1.93 \times 10^{-5}$  at 90% confidence level.

## I. Introduction

Hadron spectroscopy is a unique way to access quantum chromodynamics(QCD). Given many recent processes, our present baryon spectroscopy is still in its infancy[1]. Many fundamental issues in baryon spectroscopy are still not well understood[2]. Charmonium decays provide an excellent place for studying excited nucleons and hyperons  $-N^*$ ,  $\Lambda^*$ ,  $\Sigma^*$  and  $\Xi^*$ [3].

Many  $\Lambda$  resonances are predicted by quark model, but there are some  $\Lambda$  resonances which evidence of existence is poor[4]. The isospin conserving decay mode of  $\psi' \rightarrow X\Lambda$ ,  $X \rightarrow \bar{\Lambda}\omega$  provides a good hunting ground for the potential  $\Lambda$  excitations.

Using  $4.48 \times 10^8$   $\psi'$  events collected at BESIII, we measure the branching fractions of  $\psi' \rightarrow \Lambda\bar{\Lambda}\omega$  which is observed for the first time and would guide us to study more exclusive channels and search for intermediate states of  $\Lambda^* \rightarrow \Lambda\omega$  or  $\bar{\Lambda}^* \rightarrow \bar{\Lambda}\omega$ .

## II. BESII detector and Monte Carlo simulation

The Beijing Electron Positron Collider II (BEPCII) is a double-ring  $e^+e^-$  collider designed to operate in the  $\tau$ -charm region with an achieved luminosity of  $10^{33} \text{ cm}^{-2}\text{s}^{-1}$  at the center-of-mass energy of 3.686 GeV. The BESIII detector has a geometrical acceptance of 93% of  $4\pi$  immersed in a magnetic field of 1.0 T[5]. The BESIII detector is composed of a helium-based main drift chamber (MDC), a plastic scintillator Time-of-flight system (TOF), a CsI (Tl) electromagnetic calorimeter (EMC) and a muon system (MUC) made of resistive plate chambers (RPC). The charged particle momentum resolution is 0.5% at 1 GeV/ $c^2$  and the energy-loss ( $dE/dx$ ) resolution is better than 6%. The time resolution of TOF is 80 ps (110 ps) in the barrel (end-caps) detectors. The photon energy resolution is 2.5% (5%) at 1.0 GeV in the barrel (end-caps) of the EMC. The spatial resolution in the MUC is better than 2 cm.

A GEANT4-based[6] Monte Carlo (MC) simulation package is used to determine the detection efficiency, optimize event criteria and estimate backgrounds. The  $\psi'$  resonance is generated by KKMC[7], where the known decay modes are generated by EvtGen[8] with BF(Branching fraction) set to the world average values[4] and the remaining decays are generated by Lundcharm model[9]. The analysis is based on a sample of  $4.48 \times 10^8$   $\psi'$  events collected with the BESIII detector operating at the BEPCII collider in 2009 and 2012, and the software framework used for the data analysis is BESIII Offline Software System (Boss). The Boss version is 6.6.4.p03. An inclusive MC sample of  $5.06 \times 10^8$   $\psi'$  events is used to investigate possible background. And an exclusive MC samples of  $1.0 \times 10^6$   $\psi'$  events is generated to optimize the selection criteria and determine the corresponding selection efficiencies.

## III. Event selection

The decay  $\psi' \rightarrow \Lambda\bar{\Lambda}\omega$  is reconstructed from cascade decays  $\Lambda \rightarrow p\pi^-$ ,  $\bar{\Lambda} \rightarrow \bar{p}\pi^+$ ,  $\omega \rightarrow \pi^+\pi^-\pi^0$  and  $\pi^0 \rightarrow \gamma\gamma$ .

Charged-particle tracks in the polar angle range  $|\cos\theta| < 0.93$  are reconstructed hits from the MDC. For the pions decay from  $\omega$ , tracks with their points of closest approach

to the beamline within 10 cm of the interaction point in the beam direction, and within 1 cm in the plane perpendicular to the beam are selected. The number of charged tracks is required to be 6, the net charge of the event is 0. TOF and  $dE/dx$  information are combined to determine particle identification confidence levels for  $\pi$ , K and p hypotheses; and the particle type with highest confidence level is assigned to each track. To identify a track is a pion, it is required  $Prob(\pi) > Prob(p)$  and  $Prob(\pi) > Prob(K)$ . The  $\pi^+$  and  $\pi^-$  decay from  $\omega$  are required to be identified. There is no PID (particle identification) requirement on the proton and pion decay from  $\Lambda$  and  $\bar{\Lambda}$ . The decay product of  $\Lambda$  ( $\bar{\Lambda}$ ) with larger  $Prob(p)$  is assigned as proton (antiproton).

We loop all positive and negative charged tracks through second vertex fit to reconstruct  $\Lambda\bar{\Lambda}$  and select a pair of  $\Lambda$  and  $\bar{\Lambda}$  with the minimal value of  $((m_\Lambda - M_\Lambda)^2 + (m_{\bar{\Lambda}} - M_{\bar{\Lambda}})^2)$  in all combinations, where  $M_\Lambda$  and  $M_{\bar{\Lambda}}$  are the mass of reconstructed  $\Lambda$  and  $\bar{\Lambda}$ ,  $m_\Lambda$  and  $m_{\bar{\Lambda}}$  are the mass of  $\Lambda$  and  $\bar{\Lambda}$  in PDG. There's no further requirement on the  $\chi^2$  and decay length of the second vertex fit for the  $\Lambda/\bar{\Lambda}$  candidate.

Photon candidates are reconstructed by clustering signals in EMC crystals. The photon candidates are required to be in the barrel region ( $|\cos\theta| < 0.8$ ) of the EMC with at least 25 MeV energy deposition, or in the endcaps region ( $0.8 < |\cos\theta| < 0.92$ ) with at least 50 MeV energy deposition, where  $\theta$  is the polar angle of the shower. The timing obtained from the EMC is required to be  $0 \leq t_{EMC} \leq 700$  ns to suppress electronic noise and energy depositions that are unrelated to the event. To suppress showers generated by charged particles, the photon candidates are furthermore required to be separated by an angle larger than  $10^\circ$  degree and larger than  $30^\circ$  from the proton and anti-proton, respectively. And there are no less than 2 photons with the requirements specified above.

$\pi^0$  candidates are selected from photon pairs, the selected  $\gamma\gamma$  combinations are subjected to a one constraint (1C) kinematic fit under the  $\pi^0 \rightarrow \gamma\gamma$  hypotheses, and the  $\chi^2$  of the 1C kinematic fit is required to be less than 25.

We perform a 5C (five constraint) kinematic fit with the  $\psi' \rightarrow \Lambda\bar{\Lambda}\pi^+\pi^-\pi^0$  hypothesis with  $\gamma\gamma$  constrained to  $\pi^0$  decay. If there is more than one candidates, the combination with the smallest  $\chi^2$  will be selected.

After the optimization with  $\frac{s}{\sqrt{s+b}}$  ( $s$  denotes the events number of signal MC, and  $s+b$  is the total events number of data), the  $\chi^2$  of 5C kinematic fit is required to be less than 40 in this analysis.

There obvious  $\Lambda$  or  $\bar{\Lambda}$  signal can be seen in invariant mass distributions of  $p\pi^-$  and  $\bar{p}\pi^+$ .  $\Lambda(\bar{\Lambda})$  candidates are selected by requiring  $|M_{p\pi^-}(\bar{p}\pi^+) - m_{\Lambda(\bar{\Lambda})}| < 5 \text{ MeV}/c^2$ , where  $M_{p\pi^-}(\bar{p}\pi^+)$  is the invariant mass of  $p\pi^-$  ( $\bar{p}\pi^+$ ) and  $m_{\Lambda(\bar{\Lambda})}$  is the nominal mass of  $\Lambda(\bar{\Lambda})$  from PDG[4]. The resulting distribution of the invariant  $M_{p\pi^-}$  versus  $M_{\bar{p}\pi^+}$  is illustrated in 1.(a).

In the recoil mass distributions of the system recoiling against  $\pi^+\pi^-$  obvious  $J/\psi$  structure can be seen, is shown in 1.(b). Backgrounds from  $\psi' \rightarrow p\bar{p}J/\psi$  are rejected  $|M_{\pi^+\pi^-}^{rec} - m_{J/\psi}| > 30 \text{ MeV}/c^2$ ,  $M_{\pi^+\pi^-}^{rec}$  is the recoil mass of the system recoiling against  $\pi^+\pi^-$  and  $m_{J/\psi}$  is the nominal mass of  $J/\psi$ .

In the process of searching for  $\Lambda^*/\bar{\Lambda}^*$ ,  $\omega$  candidates are selected by requiring  $|M_{\pi^+\pi^-\pi^0} - m_\omega| < 30 \text{ MeV}/c^2$ ,  $M_{\pi^+\pi^-\pi^0}$  is the invariant mass of  $\pi^+\pi^-\pi^0$  and  $m_\omega$  is the nominal mass of  $\omega$ .

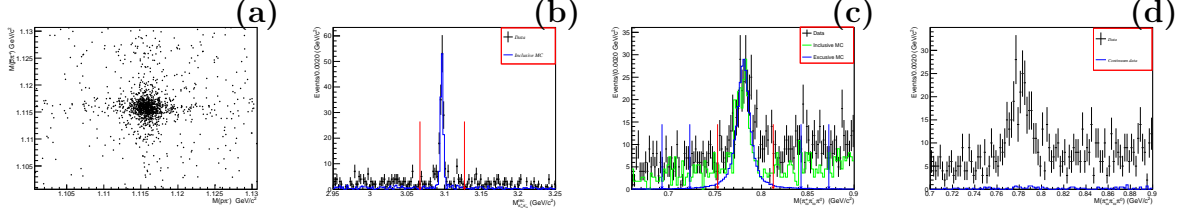


FIG. 1. (a) shows the scatter diagram of  $M_{p\pi^-}$  versus  $M_{\bar{p}\pi^+}$  from data; (b) shows the recoil mass of the system recoiling against  $\pi^+\pi^-$ , dots with error bars are from  $\psi'$  data, blue histogram comes from Inclusive MC; (c)(d) show the invariant mass distribution of  $\pi^+\pi^-\pi^0$  (c) dots with error bars are from  $\psi'$  data, green histogram comes from Inclusive MC, blue histogram comes from phase space and the blue arrow is the  $\omega$  sideband region, the red arrow is the  $\omega$  signal region. (d) the dots with error bars are from  $\psi'$  data, blue histogram shows the background estimated with the continuum data at 3.773 GeV data after the normalization

#### IV. Background analysis

To study the possible backgrounds, we analysed  $5 \times 10^8$   $\psi'$  inclusive Monte Carlo sample. After above selection requirements, signal and background events are 226 and 100, respectively. And we can find that all of those backgrounds hardly have  $\omega$  in the final state. So we can use the events in sideband region the (*bluearrow*,  $0.693 \text{ GeV} \sim 0.723 \text{ GeV}$  and  $0.843 \text{ GeV} \sim 0.873 \text{ GeV}$ ) to estimate the backgrounds in the signal region (*redarrow*,  $0.753 \text{ GeV} \sim 0.813 \text{ GeV}$ ), in Fig. 1 (c).

To study the contribution from electromagnetic process  $e^+e^- \rightarrow \Lambda\bar{\Lambda}\omega$ , we analyzed the continuum data collected at 3.65 GeV. No events pass the selection cuts. We use the data collected at 3.77 GeV instead, assuming the non-DDbar decay of  $\psi(3773) \rightarrow \Lambda\bar{\Lambda}\omega$  is negligible. Fig. 1 (d) shows the  $\psi(3773)$  events within  $\omega$  mass window after the final event selection criteria and then normalize it to  $\psi'$ . No significant  $\omega$  signal can be observed here, so we can ignore the continuous contribution of electromagnetic process  $e^+e^- \rightarrow \Lambda\bar{\Lambda}\omega$  in the background.

#### V. Branching fraction measurement

Fig 2 shows the results of the fitting  $\omega$  mass distributions. Unbinned maximum likelihood method is adopted. The signal probability density function (PDF) is described by a RooKeys PDF of the signal MC and the background is described by a first order Chebyshev polynomial. Branching fraction of  $\psi' \rightarrow \Lambda\bar{\Lambda}\omega$  can be written as:  $B(\psi' \rightarrow \Lambda\bar{\Lambda}\omega) = \frac{N_{obs}}{N_{\psi'} \cdot B(\Lambda \rightarrow p\pi^-) \cdot B(\bar{\Lambda} \rightarrow \bar{p}\pi^+) \cdot B(\omega \rightarrow \pi^+\pi^-\pi^0) \cdot B(\pi^0 \rightarrow \gamma\gamma) \cdot \varepsilon}$ , where  $N_{obs}$  is the number of the observed events, which is yielded by fitting the invariant mass spectrum of  $\omega$  after the final event selection.  $N_{\psi'} = (448 \pm 2.9) \times 10^6$  is the total number of the  $\psi'$  events.  $\varepsilon$  is detection efficiency estimated by MC simulation, which is  $(3.79 \pm 0.02)\%$ .  $B(\Lambda \rightarrow p\pi^-)$ ,  $B(\bar{\Lambda} \rightarrow \bar{p}\pi^+)$ ,  $B(\omega \rightarrow \pi^+\pi^-\pi^0)$  and  $B(\pi^0 \rightarrow \gamma\gamma)$  are the Branching fractions corresponding decays quoted from PDG[4], respectively. The yield of  $\omega$  is  $209 \pm 21$ . The measurement of  $B(\psi' \rightarrow \Lambda\bar{\Lambda}\omega)$  is  $(3.42 \pm 0.34(stat.)) \times 10^{-5}$ . The error is statistical only.

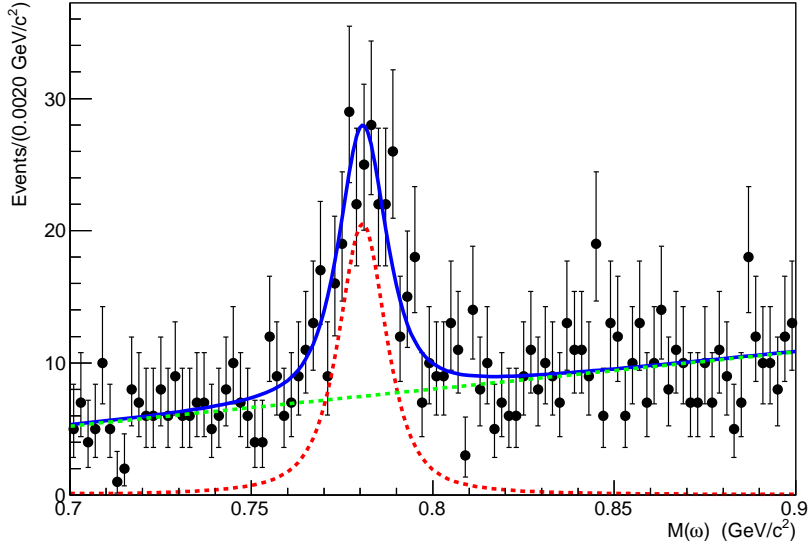


FIG. 2. Fitting results of  $M_{\pi^+\pi^-\pi^0}$ . Dots with error bars are data, the blue curve is the fitting results, the red dotted curve is the omega signal, the green dotted curve is the background pdf.

## VI. Search for $\Lambda^*/\bar{\Lambda}^*$

### A. Signal shape

The  $\Lambda^*$  resonances can be described by a S-Wave Breit-Wigner function. The 2-Dimensional signal PDF can be expressed as  $\epsilon(x, y) \cdot (\frac{p \cdot q}{(M_R^2 - x)^2 + M_R^2 \Gamma^2} + \frac{p \cdot q}{(M_R^2 - y)^2 + M_R^2 \Gamma^2}) \otimes \sigma(x, y)$ , where  $x, y$  is the spectra of  $M^2(\Lambda\omega)$  and  $M^2(\bar{\Lambda}\omega)$ , respectively;  $M_R$  and  $\Gamma$  are the mass and width of  $\Lambda^*/\bar{\Lambda}^*$ ;  $p$  is the momentum of  $\Lambda^*/\bar{\Lambda}^*$  in the c.m. frame;  $q$  is the momentum of  $\omega$  in the rest frame of  $\Lambda^*/\bar{\Lambda}^*$ . The definition of the momentum of particle 1(2) in the rest frame of particle with mass  $M$ , which decays into two particles with mass  $m_1$  and  $m_2$   $:|p_1| = |p_2| = \frac{\sqrt{(M^2 - (m_1 + m_2)^2)(M^2 - (m_1 - m_2)^2)}}{2M}$ ;  $\sigma$  is the Gaussian resolution function for  $x$  and  $y$ , obtained from a zero width  $\Lambda^*$  and  $\bar{\Lambda}^*$  signal MC;  $\epsilon(x, y)$  is the 2-Dimensional detection efficiency of  $x$  and  $y$ , which is obtained from  $\psi' \rightarrow \Lambda\bar{\Lambda}\omega$  exclusive MC.

### B. Background shape

The background can be composed of two parts,

- The non-resonant contribution is described by PHSP MC, which is floating in the fit.
- The non-omega background is described by the normalized  $\omega$  sidebands, which is fixed in the fit.

### C. Fitting result of a hypothetical $\Lambda^*/\bar{\Lambda}^*$ resonance

An unbinned maximum likelihood fit is performed to data. The projection of 2-dimensional fitting results is shown in Fig 3, where the dots represent data, the red dotted line is the signal shape, the green dotted line is the background described by  $\omega$  sideband and blue line is the background described by PHSP MC. The fitted  $\Lambda^*/\bar{\Lambda}^*$  parameters are  $M_{\Lambda^*/\bar{\Lambda}^*}=2.001 \pm 0.007 \text{ GeV}/c^2$ ,  $\Gamma_{\Lambda^*/\bar{\Lambda}^*}=0.036 \pm 0.014 \text{ GeV}/c^2$ , and the signal yields is  $51 \pm 16$  with a significance of  $3.3\sigma$ . And the goodness of fit ( $\chi^2/bin$ ) for  $M_{\Lambda\omega}^2$  and  $M_{\Lambda\omega}^2$  is 1.12 and 0.46, respectively.

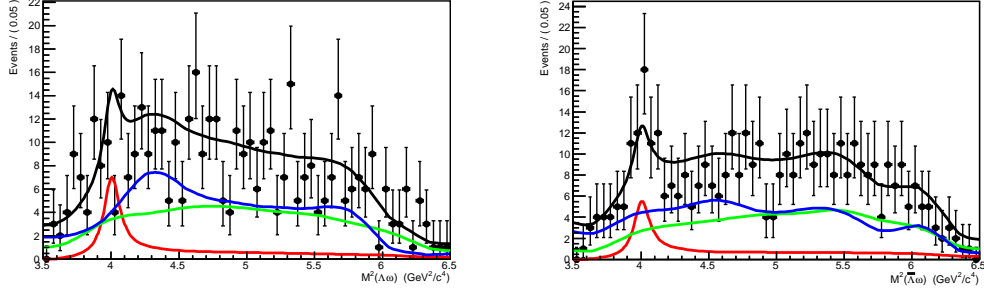


FIG. 3. The fitting results of a 2-Dimensional fit to the Dalitz plot of  $\psi(3686) \rightarrow \Lambda\bar{\Lambda}\omega$ . Dots with error bars are data, the black curve is the fitting results, the red curve is the  $\Lambda^*/\bar{\Lambda}^*$  signal, the green curve is the  $\omega$  phase space background pdf and the blue curve is the  $\omega$  sideband background pdf.

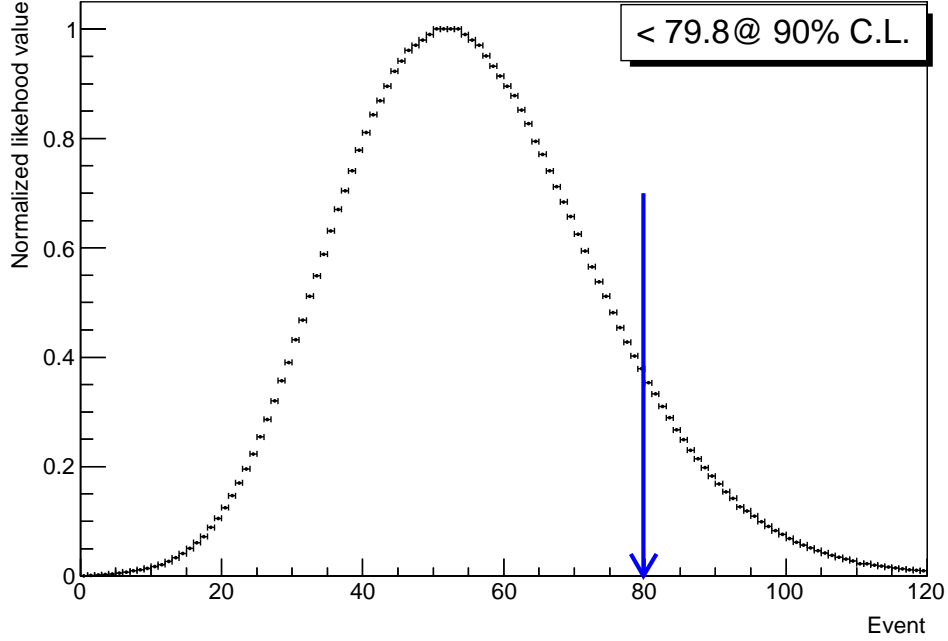


FIG. 4. The curve of Normalized likelihood value versus number of signal

## D. Upper limit of $\Lambda^*/\bar{\Lambda}^*$

In this analysis, we use a Bayesian method to calculate obtain the upper limit of the branching fraction of  $\psi' \rightarrow \Lambda\bar{\Lambda}^*/\bar{\Lambda}\Lambda^* \rightarrow \Lambda\bar{\Lambda}\omega$ . We perform the fit many times with different hypothesis of signal number, and the corresponding normalized likelihood values can be obtained. The upper limit of the signal yields at the 90% confidence level(C. L.) is defined as  $N_{UL}$ , corresponding to the number of events at 90% of the integral of the probability density function(PDF).The curve of normalized likelihood value versus number of signal is plotted in Fig 4.

The upper limit branching fractions of  $\psi' \rightarrow \Lambda\bar{\Lambda}^*/\bar{\Lambda}\Lambda^* \rightarrow \Lambda\bar{\Lambda}\omega$  is calculated as follows: $B(\psi' \rightarrow \Lambda\bar{\Lambda}^*/\bar{\Lambda}\Lambda^* \rightarrow \Lambda\bar{\Lambda}\omega) < \frac{N_{UL}}{N_{\psi'} \times B(\Lambda \rightarrow p\pi^-) \times B(\bar{\Lambda} \rightarrow \bar{p}\pi^+) \times B(\omega \rightarrow \pi^+\pi^-\pi^0) \times B(\pi^0 \rightarrow \gamma\gamma) \times \varepsilon}$ , where  $N_{UL}$  is the number of the observed signal events extracted from the fit to the daliz plot ( $M_{\Lambda\omega}^2$  vs  $M_{\bar{\Lambda}\omega}^2$ ) for the decay mode of  $\psi' \rightarrow \Lambda\bar{\Lambda}\omega$ ,  $N_{\psi'}$  is the number of  $\psi'$ [7],  $\varepsilon$  is the MC-determined detection efficiency.  $B(\Lambda \rightarrow p\pi^-)$ ,  $B(\bar{\Lambda} \rightarrow \bar{p}\pi^+)$ ,  $B(\omega \rightarrow \pi^+\pi^-\pi^0)$  and  $B(\pi^0 \rightarrow \gamma\gamma)$  are the branching fraction of  $\Lambda \rightarrow p\pi^-$ ,  $\bar{\Lambda} \rightarrow \bar{p}\pi^+$ ,  $\omega \rightarrow \pi^+\pi^-\pi^0$  and  $\pi^0 \rightarrow \gamma\gamma$  quoted from the PDG[10],respectively.

To take into account the systematic uncertainties related to the fits, alternative fits with different  $\omega$  sideband background level and shape are performed. We study the uncertainty of background level by changing the number of fixed background event by one standard deviation of statistical uncertainty. We study the uncertainty of background shape by varying the region of  $\omega$  sidebands. The maximum upper limit of the signal yields  $N_{UL}$  among these cases is chosen to calculate the upper limit of branching fraction at 90% confidence level. The maximum number of signal is 79.8. The upper limit branching fraction is calculated to be  $Br(\psi' \rightarrow \Lambda\bar{\Lambda}^*/\bar{\Lambda}\Lambda^* \rightarrow \Lambda\bar{\Lambda}\omega) < 1.93 \times 10^{-5}$ .

## VII. Systematic uncertainties

- $\psi'$  total number. The uncertainty due to the number of  $\psi'$  events is 0.65%.[10]
- MDC tracking and PID efficiency. The uncertainty of the tracking efficiency is taken to be 1.0% per track, and we take 6.0% for total uncertainty of tracking efficiency in our analysis. The average PID efficiency difference between data and MC is 2.0% per charged particle and %4.0 is taken as the systematic uncertainty for two charged tracks to reconstruct  $\pi^0$ . [11][12]
- $\Lambda/\bar{\Lambda}$  and  $\pi^0$  reconstruction. The  $\Lambda/\bar{\Lambda}$  reconstruction have been studied in the decay  $\psi' \rightarrow \Lambda\bar{\Lambda}\eta$ , which has same final state of  $\psi' \rightarrow \Lambda\bar{\Lambda}\omega$ [13]. In this study we take 2.0% as  $\Lambda/\bar{\Lambda}$  reconstruction. The uncertainty of the  $\pi^0$  reconstruction from  $\gamma\gamma$  final state is 1.0% per  $\pi^0$ , which is determined from a high purity control sample of  $J/\psi \rightarrow p\bar{p}\pi^0$ . [14]
- Photon detection efficiency. The uncertainty in the photon reconstruction is studied by using the control sample  $J/\psi \rightarrow \rho^0\pi^0$ , and a 1.0% systematic uncertainty is estimated for each photon.[15] As there are two photons in the decay final state of  $\psi' \rightarrow \Lambda\bar{\Lambda}\omega$ , the photon detection efficiency is determined to be 2.0%.
- Kinematic Fit. The systematic uncertainty due to kinematic fitting is estimated by correcting the helix parameters of charged tracks according the method described in Ref.[12].

Difference in the detection efficiency between with and without correction to the MC samples is taken as the uncertainty.

- Intermediate decay. The systematic uncertainties on the intermediate-decay  $\Lambda \rightarrow p\pi^-$ ,  $\bar{\Lambda} \rightarrow \bar{p}\pi^+$ ,  $\omega \rightarrow \pi^+\pi^-\pi^0$  and  $\pi^0 \rightarrow \gamma\gamma$  are quoted from PDG[4].

- Mass window. The systematic error of ( $M_{p\pi^-}$ ,  $M_{\bar{p}\pi^+}$ , and  $M_{\pi^+\pi^-\pi^0}$ ) mass window cut is due to the different mass resolution of them between data and signal MC. We use a gauss function smear the signal MC shape to get a better consistent with data, and the difference of the MC detection efficiency before and after smear is taken as the systematic uncertainties from this item. The uncertainty from  $J/\psi$  veto is estimated by varying the mass window cut, the alternative fit with different  $J/\psi$  mass window is performed.

- Fitting

For the measurements of  $\psi' \rightarrow \Lambda\bar{\Lambda}\omega$  branching fraction .

- Signal shape

The signal shape in measure branching fraction of  $\psi' \rightarrow \Lambda\bar{\Lambda}\omega$  is described by a RooKeys PDF of the signal MC. A fit is performed by using a RooKeys PDF of the signal MC convolutes a Gaussian function as the signal pdf and take the different as the systematic error, which is 2.9 percent

- Background shape

The description of backgrounds in measure branching fraction of  $\psi' \rightarrow \Lambda\bar{\Lambda}\omega$  is described by a first order Chebyshev polynomial. There is a second order Chebyshev polynomial as the background pdf and take the different as the systematic error, which is 1.4 percent

- Fitting range

Changing the fit range and taking the difference as the uncertainty which is 1.5 percent.

source	$\psi' \rightarrow \Lambda\bar{\Lambda}\omega$	Upper limit of $\Lambda^*/\Lambda^*$
Number of $\psi'$ events	0.65%	0.65%
MDC tracking	6%	6%
PID	4%	4%
$\Lambda/\bar{\Lambda}$ reconstruction	2%	2%
$\pi^0$ reconstruction	1%	1%
Good photon	2%	2%
Kinematic Fit	1.7%	1.7%
Intermediate decay	$\Lambda \rightarrow p\pi^-$	0.8%
	$\bar{\Lambda} \rightarrow \bar{p}\pi^+$	0.8%
	$\omega \rightarrow \pi^+\pi^-\pi^0$	0.8%
	$\pi^0 \rightarrow \gamma\gamma$	0.03%
Mass window	$M_\Lambda$	0.02%
	$M_{\bar{\Lambda}}$	0.03%
	$M_{\pi^+\pi^-}^{rec}$	1.6%
	$M_\omega$	— — —
	Signal shape	2.9%
Fitting	Background shape	1.4%
	Fitting range	1.5%
Total	9.1%	8.3%

TABLE I. Summary of systematic uncertainties



209 Tab I demonstrates the possible systematic error sources and their fractional contribution  
 210 to the measurement of  $\psi' \rightarrow \Lambda \bar{\Lambda} \omega$  branching fraction and upper limit of  $\Lambda^*/\bar{\Lambda}^*$ .

## 211 A. Result

212 The branching fraction of  $\psi' \rightarrow \Lambda \bar{\Lambda} \omega$  is  $(3.42 \pm 0.34(stat.) \pm 0.31(syst.)) \times 10^{-5}$ .

213 To conservatively estimate the upper limit of branching fractions, the multiplicative un-  
 214 certainties are considered by smearing the normalized likelihood curve with a Gaussian func-  
 215 tion  $G(\mu, \sigma) = G(0, \sigma_{sys})$ ,  $\sigma_{sys} = N * \sigma_{rel}$ ,  $\sigma_{rel} (= 8.3\%)$  is the corresponding combined relativ-  
 216 ity uncertainty and N is the input signal yield:  $L(N') = \int_0^\infty L(N) \frac{1}{\sqrt{2\pi}\sigma_{sys}} \exp[-\frac{(N'-N)^2}{2\sigma_{sys}^2}] dN$ ,  
 217 where L(N) is the normalized likelihood distribution obtained from fitting the curve of nor-  
 218 malized likelihood value vs signal number and parameterized as a Gaussian function.

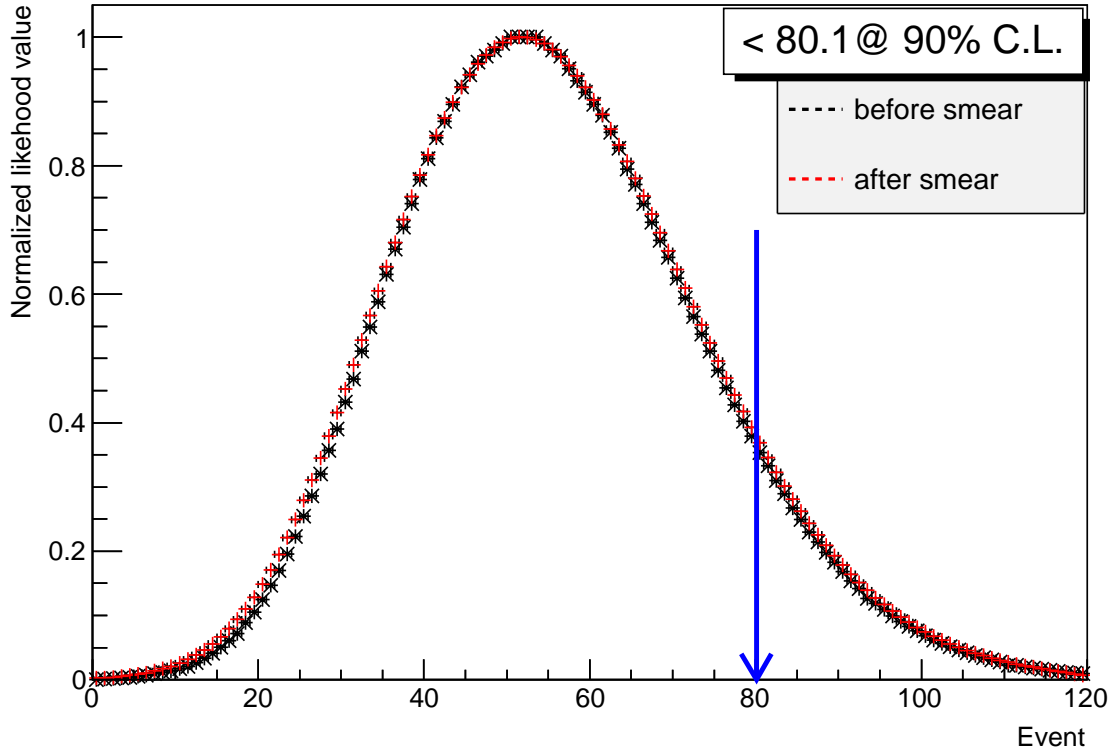


FIG. 5. Normalized likelihood distribution before (black dot) and after (red dot) convolution.

219 The Fig 5 shows the likelihood distribution before and after smearing. In this way,  
 220 the upper limit of the branching fraction at the 90% confidence level is determined to be  
 221  $1.93 \times 10^{-5}$

## VIII. Summary

Using a sample of  $4.48 \times 10^8$   $\psi'$  events collected with BESIII detector at BEPCII storage ring taken in the year 2009 and 2012, at center-of-mass energy  $\sqrt{s} = 3.686 \text{ GeV}/c^2$ , the measurement of  $\psi' \rightarrow \Lambda \bar{\Lambda} \omega$  is analyzed, which is observed for the first time, and the branching fraction of  $\psi' \rightarrow \Lambda \bar{\Lambda} \omega$  is measured to be  $(3.42 \pm 0.34(\text{stat.}) \pm 0.31(\text{syst.})) \times 10^{-5}$ . A search for the decay  $\psi' \rightarrow \bar{\Lambda}^* \Lambda / \Lambda^* \bar{\Lambda} \rightarrow \Lambda \bar{\Lambda} \omega$  is performed via the process  $\psi' \rightarrow \Lambda \bar{\Lambda} \omega$ . There is no evidence of any  $\Lambda^*$  in both invariant mass distributions. However a 2-dimensional fit to the Dalitz plot of  $\psi' \rightarrow \Lambda \bar{\Lambda} \omega$  gives a mass of  $2.001 \pm 0.007 \text{ GeV}/c^2$  and width is  $0.036 \pm 0.014 \text{ GeV}/c^2$  with the significance of  $3.3\sigma$ . The corresponding upper limit of  $Br(\psi' \rightarrow \bar{\Lambda}^* \Lambda / \Lambda^* \bar{\Lambda} \rightarrow \Lambda \bar{\Lambda} \omega)$  is measured as  $1.93 \times 10^{-5}$  at C.L. of 90%.

- 
- [1] J. Beringer et al. [Particle Data Group Collaboration], Review of Particle Physics (RPP), Phys. Rev. D 86, 010001 (2012).
  - [2] S. Capstick, S. Dytman, R. Holt, X. -d. Ji, J. W. Negele, E. Swanson, P. Barnes and T. Barnes et al., Key issues in hadronic physics, [hep-ph/0012238]. E. Klempt and J. -M. Richard, Baryon spectroscopy, Rev. Mod. Phys. 82, 1095 (2010).
  - [3] B. -S. Zou,  $\Lambda^*$ ,  $\Sigma^*$  and  $\Xi^*$  resonances from J /  $\Psi$  and  $\Psi$ -prime decays, Nucl. Phys. A 684, 330 (2001).
  - [4] M. Tanabashi et al. (Particle Data Group), Phys. Rev. D 98, 030001 (2018).
  - [5] M. Ablikim et al. (BES Collaboration), Nucl. Instrum. Methods Phys. Res. Sect. A 614, 345 (2010).
  - [6] S. Agostinelli et al. (GEANT4 Collaboration), Nucl. Instrum. Methods Phys. Res. Sect. A 506, 250 (2003).
  - [7] S. Jadach, B. Ward, and Z. Was, Phys. Rev. D 63, 113009 (2001).
  - [8] D. J. Lange, Nucl. Instrum. Methods Phys. Res. Sect. A 462, 152 (2001).
  - [9] J. C. Chen, G. S. Huang, X. R. Qi, D. H. Zhang, and Y. S. Zhu, Phys. Rev. D 62, 034003 (2000).
  - [10] M. Ablikim et al. (BES Collaboration), arXiv:1709.03653.
  - [11] M. Ablikim et al. (BES Collaboration), Phys. Rev. D 87, 012007 (2013).
  - [12] M. Ablikim et al. (BES Collaboration), Phys. Rev. D 87, 012002 (2013).
  - [13] M. Ablikim et al. (BES Collaboration), Phys. Rev. D 87, 052007 (2013).
  - [14] M. Ablikim et al. (BES Collaboration), Phys. Rev. Lett. 105, 261801 (2010).
  - [15] M. Ablikim et al. (BES Collaboration), Phys. Rev. D 81, 052005 (2010).